Verification of a displacement model for three-point bending test

Kožar, I.; Sulovsky, T.; Plovanić, M.; Božić, Ž.

Available online at www.sciencedirect.com

ScienceDirect

Procedia Structural Integrity 46 (2023) 143–148

Structural Integrity Procedia

www.elsevier.com/locate/procedia

5th International Conference on Structural Integrity and Durability

Verification of a displacement model for three-point bending test

I. Kožar[a]*, T. Sulovsky[a], M. Plovanić[a], Ž. Božić[b]

[a]*University of Rijeka, Faculty of Civil Engineering, R. Matejčić 3, 51000 Rijeka, Croatia*
[b]*University of Zagreb, Faculty of Mech. Eng. And Nav. Arch., I. Lučića 5, 10000 Zagreb, Croatia*

Abstract

Three-point bending is an important test for various parameters in materials science, and the complete test yields a force-displacement diagram. In this work, we have developed a numerical model that can describe the testing process and help us to determine relevant material properties related to the fracture process. The novel numerical model includes a parameter that is determined using an inverse analysis, which is described in this paper. The validity of the model is confirmed by comparing the measured data and the calculated values.

Keywords: three-point bending; force-displacement; post-peak behavior; crack propagation; inverse model;

Nomenclature

P_m	experimentally measured force from the force - displacement diagram
δ_m	experimentally measured displacement from the force - displacement diagram
κ	parameter for control of the singularity in the model
τ	pseudo-time
Y_0	displacement function describing deflection in the three-point test

* Corresponding author.
E-mail address: ivica.kozar@gradri.uniri.hr

10.1016/j.prostr.2023.06.024

1. Introduction

Three-point bending is an important test for various parameters in materials science. The complete test results in a force-displacement diagram that covers both the pre-peak and post-peak behaviour of the beam. The pre-peak data provides information on the elastic material properties, the determination of which is a routine task. The post-peak data provide information about the material properties related to fracture. In this work, we have developed a numerical model to describe the testing procedure and to help us determine the relevant material properties related to the fracture process. In our previous work, we developed a simple layered model for the correlation between the load (force) and the vertical displacement Kožar et al. (2021). In Kožar et al. (2020), we presented stochastic properties of load-displacement curves resulting from three-point bending tests. Some inverse methods for extraction of material parameters are presented in Kožar et al.(2018), Menke(2012) and Čakmak et al (2021). The extension of the analysis to fibre-reinforced concrete is presented in Kožar et al. (2019) and Rukavina et al. (2019). The evolution of cracks in brittle and quasi-brittle materials and the associated failure is presented in Voznesenskii et al. (2017), Mlikota et al. (2021), Gljušćić et al. (2021), Liović et al. (2021), Vukelić et al. (2021), Pastorčić et al. (2019). All calculations are performed in Wolfram Mathematica Wolfram Mathematica (2021).

2. Formulation of the forward problem

The bending of the three-point specimen can be considered as a beam bending problem up to the point where no cracks occur. Thereafter, we assume that the beam shape changes as the crack propagates through the beam. The geometry of the problem is shown in Fig.1

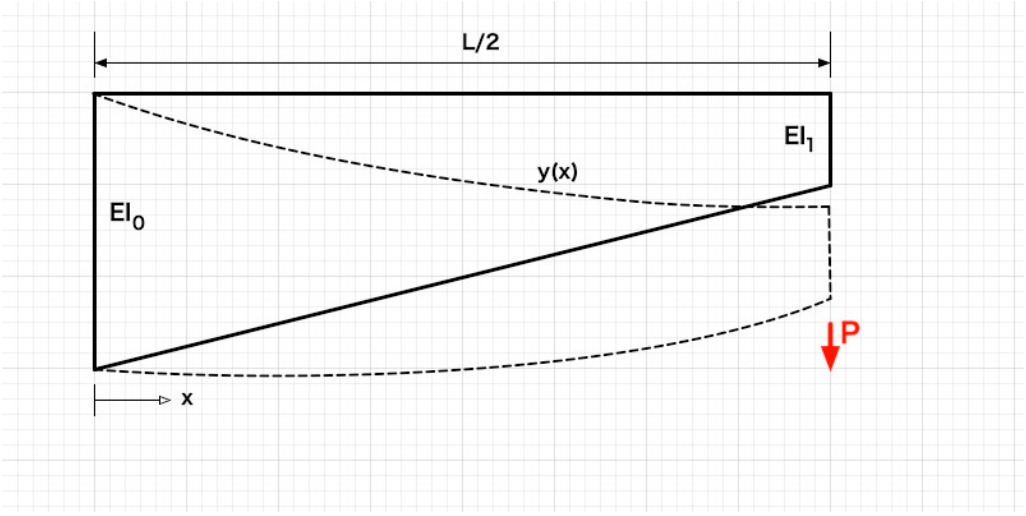

Fig. 1. Beam model for displacement.

Our forward model is an extended beam bending model that can be described by the following differential equation

$$y''(x) + \frac{M(x)}{EI(x)} = 0 \tag{1}$$

with b.c. $y(x = 0) = 0$ and $y'(x = {}^{L}/_{2}) = 0$. Here

$$EI(x) = EI_0 - \Delta EIx\,, \qquad \Delta EI = \frac{EI_0 - EI_1}{{}^{L}/_{2}} \tag{2}$$

We develop $\frac{P}{EI_0-\Delta EIx}$ into a series and take the first two members of the series and introduce $P_0 = {}^{P}/_{EI_0}$, $P_1 = {}^{P\,\Delta EI}/_{EI_0^2}$, etc., we can rewrite the differential equation

$$y''(x) + P_0 + P_1 x = 0 \tag{3}$$

Solution of this differential equation is

$$y(x) = \frac{x}{24}(12LP_0 + 3L^2P_1x - 12P_0x^2 - 4P_1x^3) \tag{4}$$

The standard displacement model results from the solution of the beam differential equation and is valid only in the elastic range, i.e., up to the peak load. We have performed calculations with three and four series members, but this does not significantly change the later results.

2.1. Beam displacement with singularity

It should be noted that this solution does not propagate even when $\Delta EI \rightarrow 0$, and therefore is suitable only for the first part of the load before crack initiation. The solution is to introduce a parameter that somehow controls the singularity of the solution, and we introduce a

$$\Delta EI(\kappa) = 2\,EI_0\left(1-\frac{\kappa}{L}\right) \tag{5}$$

Therefore, an additional term was added to the standard solution, as shown in equation (6)

$$Y_0(P,\kappa) = \frac{P}{48}\left(\frac{2L^3}{EI_0}\left(1-\frac{\kappa}{L}\right)+\frac{3L^2}{EI_0}\right) + \frac{1-\kappa}{\kappa} \tag{6}$$

Now, the solution can become singular for certain values of the parameter κ and is also a function of this parameter. We could say that the parameter κ describes the position of the crack depth. When $\kappa = 1$, there is no change in the elastic solution. The crack depth changes, so κ must also change during the loading process. Changes could be introduced if we introduce the 'pseudo-time' τ (the pseudo-time is a known parameter in our three-point bending test) and $\kappa \equiv \kappa(\tau)$.

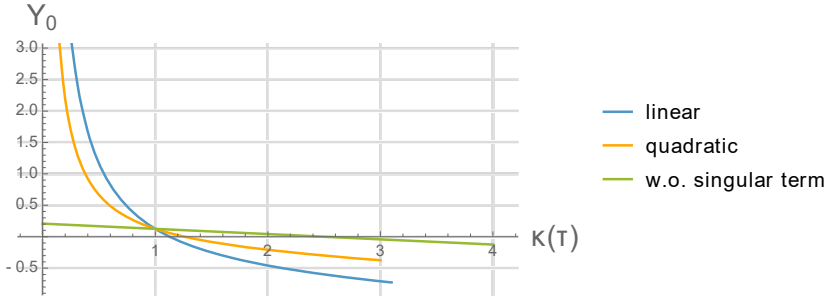

Fig. 2. Influence of the parameter $\kappa(\tau)$ as pseudo-time changes in the interval $\tau \in (0, 1]$.

In Fig.2 we have shown the meaning of the parameter $\kappa(\tau)$ and the necessity of an additional singular term. Equation (6) is called the 'forward' model and has two parameters, the force 'P' and the fracture parameter $\kappa(\tau)$. Only for the correct values of the fracture parameter $\kappa(\tau)$ we obtain the inverse model, which is able to reproduce the data measured in the experiment.

2.2. Displacement measurement

The results of a real laboratory experiment are shown in Fig.3.

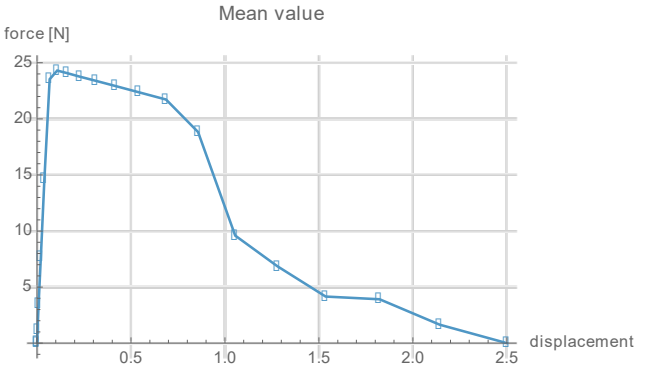

Fig. 3. Measured force - displacement diagram.

From the above results, it is easy to extract data for the force change in pseudo-time and for the displacement change in pseudo-time. After that, it is only necessary to substitute the measured force P_m, δ_m into equation (6) and obtain the (correct) displacements. However, to obtain correct results, one must know the corresponding parameter $\kappa(\tau)$.

3. Model for inverse analysis

Equation (6) is called a "forward model" because it relates two basic model values, the force "P" and the fracture parameter $\kappa(\tau)$, but only for appropriate values of the fracture parameter $\kappa(\tau)$ does the equation reproduce the data measured in experiment. We need to formulate an inverse model capable of determining the required parameter. The correct values are obtained by solving the following nonlinear equation:)

$$Y_0(P_m, \kappa_{inv}) = \delta_m \tag{7}$$

where P_m, δ_m are measured force and displacement (from the three-point experiment), respectively.

The background of the above process could be explained by assuming the existence of a duality form Marchuk (1995), where $\int (u^* A u)\, dx = \int (u A^* u^*)\, dx$. For our problem, this gives $Y_0(P_m, \kappa) = Y_0\big(P_m, K(\tau)\big)$ with $K(\tau) \equiv \kappa$, which follows from $K(\tau) = \kappa$, but first τ is computed as the solution of equation (7). This equation can only be solved if we assume $K(\tau)$, where the particular form of the function $K(\tau)$ is not important. It only needs to be easy to manipulate and satisfy the boundary conditions, i.e., be well defined in the interval of interest.

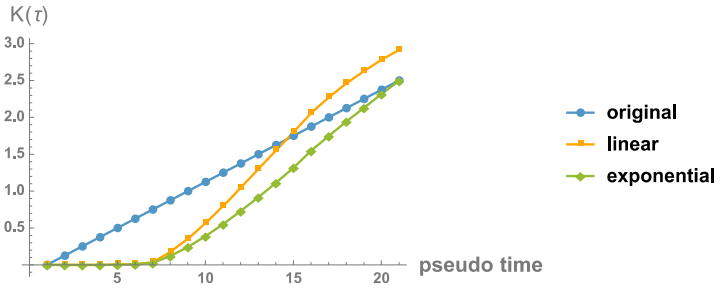

Fig. 4. Comparison of the behavior of assumed functions K(τ).

We tried two functions: one linear and one exponential. We made the choice based on how well they satisfy the boundary conditions imposed by the experiment. Their comparison is shown in Fig.4.

It can be seen from Fig.4 that the linear assumption would be an oversimplification, since the function values exceed the maximum measured displacement $\delta_m = 2.5$ mm.

The kappa parameter is calculated from $K(\tau) = \kappa$ and is shown in Fig.5.

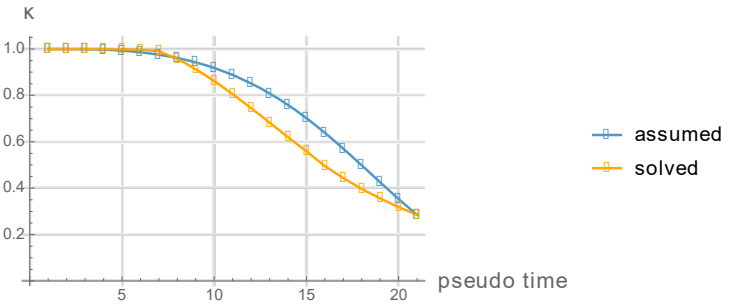

Fig. 5. Assumed and calculated parameter κ.

The resulting κ is substituted into the displacement equation (6) and yields displacements corresponding to those measured, as shown in Fig.6.

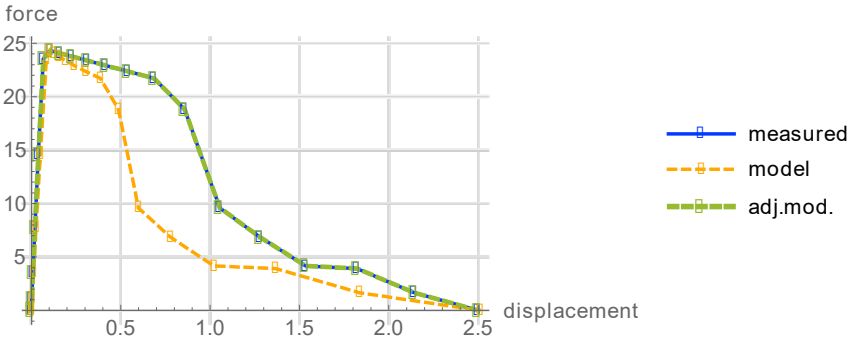

Fig. 6. Comparison of the measured and calculated displacements.

In Fig.6, the blue line represents the measured values of P_m, δ_m, the green line is the line calculated from equation (6) with the parameter κ determined from equation (7), and the orange line is that from equation (6) with the assumed parameter κ (as in Fig.5).

4. Conclusion

We have presented a method capable of numerically reproducing the force-displacement diagram obtained in three-point bending tests. The method is based on a beam bending equation extended by a singular term and on an inverse analysis to determine the required parameter.

Acknowledgements

This work has been supported through project HRZZ 7926 ”Separation of parameter influence in engineering modeling and parameter identification” and project KK.01.1.1.04.0056 ”Structure integrity in energy and transportation”, which is gratefully acknowledged.

References

Beigrezaee, M.J., Ayatollahi, M.R., Bahrami, B., da Silva, L.F.M., 2019. Failure load analysis in single lap joints - effect of adherend notching. Engineering Failure Analysis 104, 75-83.

ASTMC1609/C1609M-12., 2012. Standard test method for flexural performance of fiber-reinforced concrete (using beam with third-point loading), ASTM Committee.

Čakmak, D., Tomičević, Z., Wolf, H., Božić, Ž., Semenski, D., Trapić, I., 2019. Vibration fatigue study of the helical spring in the base-excited inerter-based isolation system. Engineering Failure Analysis 104, 44-56.

Lukacs, J., 2019. Fatigue crack propagation limit curves for high strength steels based on two-stage relationship. Engineering Failure Analysis 104, 431-442.

Majidi, H.R., Torabi, A.R., Zabihi, M., Razavi, S.M.J., Berto, F., 2019. Energy-based ductile failure predictions in cracked friction-stir welded joints. Engineering Failure Analysis 104, 327-337.

Kožar, I.,Bede, N., Mrakovčić, S., Božić, Ž., 2021.Layered model of crack growth in concrete beams in bending. Procedia Structural Integrity 31, 134 – 139.

Kožar, I., Torić Malić, N., Smolčić, Ž., Simonetti, D., 2019. Bond-slip parameter estimation in fibre reinforced concrete at failure using inverse stochastic model. Engineering Failure Analysis 104, 84–95.

Kožar, I., Torić Malić, N., Simonetti, D., Božić, Ž., 2020. Stochastic properties of bond-slip parameters at fibre pull-out. Engineering Failure Analysis 111, 104478.

Kožar, I., Torić Malić, N., Rukavina, T., 2018. Inverse model for pullout determination of steel fibers. Coupled System Mechanics 7, 197–209.

Rukavina, T., Ibrahimbegovic, A., Kožar, I., 2019. Fiber-reinforced brittle material fracture models capable of capturing a complete set of failure modes including fiber pull-out. Comput Methods Appl Mech Eng 355, 157-192.

Menke, W., 2012. Geophysical Data Analysis: Discrete Inverse Theory, Academic Press Elsevier, Cambridge, Massachusetts, USA

Marchuk, G.I., 1995. Adjoint Equations and Analysis of Complex Systems. Springer – Science + Business Media, B.V.

Čakmak, D., Tomičevicć, Z., Wolf, H., Božić, Ž., Semenski, D., 2021. Explicit solution of Rice/Lalanne peak probability distribution for statistical fatigue assessment in the frequency domain. Procedia Structural Integrity. 2021; 31: 98 – 104.

Voznesenskii, A.S., Krasilov, M.N., Kutkin , Y.O., Tavostin, M.N., Osipov, Y.V., 2017. Features of interrelations between acoustic quality factor and strength of rock salt during fatigue cyclic loadings. International Journal of Fatigue 97, 70–78.

Mlikota, M., Schmauder, S., Dogahe, K., Božić, Ž., 2021. Influence of local residual stresses on fatigue crack initiation. Procedia Structural Integrity 31, 3 – 7.

Gljušćić, M., Franulović, M., Lanc, D., Božić, Ž., 2021. Digital image correlation of additively manufactured CFRTP composite systems in static tensile testing. Procedia Structural Integrity 31, 116 – 121.

Liović, D., Franulović, M., Kozak, D., 2021. Material models and mechanical properties of titanium alloys produced by selective laser melting. Procedia Structural Integrity 31, 86 – 91.

Vukelić, G., Vizentin, G., Božić, Ž., Rukavina, L., 2021. Failure analysis of a ruptured compressor pressure vessel. Procedia Structural Integrity 31, 28 – 32.

Pastorčić, D., Vukelić, G., Božić, Ž., 2019. Coil spring failure and fatigue analysis. Engineering Failure Analysis 104, 310-318.

Wolfram Research Inc., Mathematica, 2021. URL: https://www.wolfram.com/mathematica/.

Kišiček, T., Sorić, Z., 2003. Bending moment - curvature diagram for reinforced-concrete girders (in Croatian). Journal of Civil Engineering 55, 207–215.

Bede, N., Mrakovčić, S., 2020. Flexure behaviour of high strength concrete with steel and polypropilene fibres. In: 2nd International Conference on Construction Materials for Sustainable Future (in print), 15-17 April 2020, Bled, Slovenia.

Mishnaevsky, L., 2011. Hierarchical composites: Analysis of damage evolution based on fiber bundle model. Composites Sciences and Technology 71, 450-460.

Ožbolt, J., Yijun, L., Kožar, I., 2001. Microplane Model for Concrete with Related Kinematic Constraint. International journal of solids and structures, 38(16), 2683-2711.

Gomez, Q., Uenishi, K., Ionescu., I.R., 2020. Quasi-static versus dynamic stability associated with local damage models. Engineering Failure Analysis 111, 104476.

Cazin, D., Braut, S., Božić, Ž., Žigulić R., 2020. Low cycle fatigue life prediction of the demining tiller tool. Engineering Failure Analysis 111, 104457.

Arandjelović, M., Sedmak, S.A., Milović, Lj., Maksimović, A., Božić, Ž., 2020. Crack propagation in 3PB specimen made from welded joint. Procedia Structural Integrity 28, 440–445.

Ferro, P., Berto, F., 2020. The strain energy density approach applied to bonded joints. Procedia Structural Integrity 28, 19–25.

Kožar, I. and Ožbolt, J., 2010. Some aspects of load-rate sensitivity in visco-elastic microplane material model. Computers & Concrete 7, 331-346.